

# COMPLEX RE-INNervation PATTERN AFTER UNILATERAL RENAL DENERVATION IN RATS

Kristina RODIONOVA<sup>1</sup>, Christian FIEDLER<sup>1</sup>, Franziska GUENTHER<sup>3</sup>,  
Eric GROUZMANN<sup>5</sup>, Winfried NEUHUBER<sup>2</sup>, Michael J.M. FISCHER<sup>3</sup>, Christian OTT<sup>1</sup>,  
Peter LINZ<sup>1</sup>, Wolfgang FREISINGER<sup>1</sup>, Sonja HEINLEIN<sup>1</sup>, Stephanie T. SCHMIDT<sup>1</sup>, Roland  
E. SCHMIEDER<sup>1</sup>, Kerstin AMANN<sup>4</sup>, Karie SCROGIN<sup>6</sup>, Roland VEELKEN<sup>1</sup>, Tilmann  
DITTING<sup>1</sup>

<sup>1</sup>Dept. of Internal Medicine 4 - Nephrology and Hypertension, <sup>2</sup>Dept. of Anatomy I, <sup>3</sup>Dept of  
Physiology 1, <sup>4</sup>Dept. of Pathology, Friedrich-Alexander University Erlangen FAU, Germany,  
<sup>5</sup>Service de Biomédecine, Laboratoire des Catéchoalamines et Peptides, Centre Hospitalier  
Universitaire Vaudois CHUV, Lausanne, Switzerland, <sup>6</sup>Dept. of Pharmacology and  
Experimental Therapeutics, Loyola University Chicago, Stritch School of Medicine,  
Maywood, Illinois

*short title: afferent renal reinnervation*

## ***Conflict of interest and Source of Funding:***

*RV received funding from Deutsche Forschungsgemeinschaft, SFB 423,*

*TD & RV received funding from MEDTRONIC.*

word count: 8699; word count of abstract: 250; number of figures: 12

Address for correspondence:

Tilmann Ditting, MD

Department of Internal Medicine 4, Nephrology und Hypertension,

Friedrich-Alexander University Erlangen, Germany

Ulmenweg 18, 91054 Erlangen, Germany

Tel.: +49 9131 85-36314, Fax.: +49 9131 85-39202

email: Tilmann.Ditting@t-online.de

28   **Abstract**

29   Renal denervation (DNX) is a treatment for resistant arterial hypertension. Efferent  
30   sympathetic nerves regrow, but re-innervation by renal afferent nerves has only recently been  
31   shown in the renal pelvis of rats after unilateral DNX. We examined intrarenal perivascular  
32   afferent and sympathetic efferent nerves after unilateral surgical DNX.

33   Tyrosine hydroxylase (TH), calcitonin gene related peptide (CGRP) and smooth muscle actin  
34   were identified in kidney sections from 12 Sprague-Dawley rats, to distinguish afferents,  
35   efferents, and vasculature. DNX-kidneys and non-denervated kidneys were examined 1, 4 and  
36   12 weeks after DNX. Tissue levels of CGRP and norepinephrine (NE) were measured with  
37   ELISA and mass-spectrometry, respectively.

38   DNX decreased TH- and CGRP-label by 90% and 95%, respectively ( $P<0.05$ ) within one  
39   week. After 12 weeks TH- and CGRP-label returned to baseline with a shift towards afferent  
40   innervation ( $P<0.05$ ). Non-denervated kidneys showed a doubling of both labels within 12  
41   weeks ( $P<0.05$ ). CGRP content decreased by 72% [ $3.2\pm0.3$  vs.  $0.9\pm0.2$  ng/g<sub>kidney</sub>;  $P<0.05$ ] and  
42   NA by 78% [ $1.1\pm0.1$  vs.  $0.2\pm0.1$  pmol/mg<sub>kidney</sub>;  $P<0.05$ ] one week after DNX. After 12  
43   weeks, CGRP, but not NE content in DNX kidneys was fully recovered, with no changes in  
44   the non-denervated kidneys. The use of phenol in the DNX procedure did not influence this  
45   result.

46   We found morphological re-innervation and transmitter recovery of afferents within 12 weeks  
47   after DNX. Despite morphological evidence of sympathetic regrowth, NE content did not  
48   fully recover. These results suggest a long-term net surplus of afferent influence on the DNX  
49   kidney maybe contributing to the blood pressure lowering effect of DNX.

50

51   **Keywords:**

52   renal nerve ablation, morphology, peptidergic, sympathetic efferent, immunohistochemistry.

## 53     **Introduction**

54     An increasing number of studies have reported the beneficial effects of interventional renal  
55     nerve ablation in patients with treatment-resistant hypertension (1, 18, 30, 32). Though early  
56     results were promising, more recent findings have left the benefit of renal nerve ablation in  
57     some doubt (5). The rationale for renal denervation as a therapeutic intervention for treatment  
58     (40) has evolved from a broad base of experimental (9) and clinical studies (43) originating  
59     from the last century. The most successful clinical denervation studies (1, 18, 30, 32) recorded  
60     blood pressure and other clinical outcomes, but did not focus on pathophysiological  
61     mechanisms. The degree of denervation or re-innervation was not addressed or considered  
62     given the dramatic blood pressure lowering effects of the procedure. However, all of these  
63     studies lacked truly blinded observations or sham surgical controls (5).

64     Outcomes demonstrating successful denervation, such as catecholamine spillover, have only  
65     been provided in a few studies. However, it was reported that renal catecholamine spillover  
66     was not completely abolished after renal nerve ablation in humans indicating incomplete  
67     denervation (39). Despite only reduced renal catecholamine spillover, hypertension was  
68     successfully reduced. Thus, it seems that a complete and long-lasting reduction of renal nerve  
69     innervation is not necessary for the blood pressure lowering effects of renal denervation.  
70     Moreover, there is some debate about the role of sympathetic-efferent versus peptidergic  
71     afferent nerves, and whether afferents provide sympatho-inhibitory or –excitatory effects (3,  
72     8, 21).

73     An unresolved question is to what degree autonomic and sensory nerves regrow along the  
74     renal vessels following denervation (9). Re-innervation has previously been described in  
75     transplanted kidneys in humans and rodents (22, 23). Recently, a systematic morphological  
76     study in rats demonstrated that sympathetic efferent nerves reappear in the renal pelvis and  
77     parenchyma within three months of unilateral denervation. Peptidergic afferent nerve fibers  
78     reappeared in the renal pelvis, but were not described in the renal parenchyma (34).

79 We recently provided functional evidence that intrarenal afferent nerves exert tonic inhibition  
80 on contralateral sympathetic nerve activity, most likely via a substance P dependent pathway.  
81 Renal pelvic and intrarenal afferent compartments could be functionally distinguished by  
82 pharmacologic blockade of pelvic TRPV1 receptors. However, afferent-mediated  
83 sympathoinhibition was conserved following blockade of renal pelvic nerves (10). Thus, there  
84 is evidence for a functionally relevant peptidergic innervation of the renal pelvis (19), as well  
85 as the renal parenchyma (10).

86 We hypothesized that intrarenal afferent and efferent perivascular nerves regrow after renal  
87 denervation. Here, we used the method of Mulder et al. to evaluate the impact of unilateral  
88 renal denervation (34) on both the denervated- and contralateral non-denervated kidney with  
89 special focus on intrarenal perivascular nerve fibers.

90 Since we were interested in the re-innervation potential rather than long-lasting functional  
91 denervation effects we did not combine the surgical denervation with topically applied phenol  
92 as it is was done in prior studies to ensure complete denervation (26, 34). Moreover, renal  
93 nerves are located nearly exclusively in the adventitial and perivascular space (36, 42) where  
94 they are readily accessible for subtotal renal denervation by a mere surgical procedure around  
95 the renal artery. Thus, we attempted to better model the re-innervation potential that develops  
96 after subtotal clinical denervation procedures (39, 40) by foregoing the use of additional  
97 neurotoxin. However, we also assessed the impact of additional phenol application on  
98 innervation.

99 In this study, immunohistochemical analysis of renal innervation was made 1, 4 and 12  
100 weeks after unilateral surgical denervation in male Sprague-Dawley rats. Renal pelvic fibers  
101 were not investigated in the present study. Additional experiments were done to determine the  
102 effect of denervation on renal tissue content of norepinephrine and the afferent neuronal  
103 marker, calcitonin gene related peptide (CGRP).

104

## 105    **Material and Methods**

106    Animals: Male Sprague-Dawley rats (Charles River, Kisslegg, Germany) weighing 170-200g  
107    were maintained in cages at 24±2°C and fed a standard rat diet (no. C-1000, Altromin, Lage,  
108    Germany) containing 0.2% sodium by weight and were allowed free access to tap water. All  
109    procedures were performed on animals in accordance with the National Institutes of Health  
110    (NIH) Guide for the Care and Use of Laboratory Animals and were approved by the local  
111    government agency (Regierung von Mittelfranken, Ansbach, Germany).

112

113    Unilateral surgical renal denervation: Twelve rats were assigned to 3 timed groups (n=4,  
114    each), which underwent the denervation procedure 12, 4 and 1 week before  
115    immunohistological examination of the kidneys. This reverse time schedule was chosen to  
116    avoid time and storage derived sample errors. Tissue could be processed in a short period of  
117    time and in randomized order.

118    Unilateral surgical denervation of the left renal artery was performed as follows, while the  
119    right kidney was left intact: Rats were anesthetized with a mixture of O<sub>2</sub>, 50% N<sub>2</sub>O and ~1.5%  
120    Isofluran®. A left flank incision was made and the renal denervation was performed by  
121    surgically stripping the renal arteries and veins of adventitia and cutting all renal nerve  
122    bundles visible under a dissection microscope (25-40x). This procedure not only removed  
123    sympathetic-, but also sensory fibers, which course in the same nerve bundles as the  
124    sympathetic axons. In this set of experiments, we did not coat the vessels with the neurotoxin  
125    phenol, as described by others (26), since we were attempting to model the subtotal  
126    denervation that is normally achieved in clinical procedures, rather than complete renal  
127    denervation. However, we were very careful to meticulously remove the adventitial tissue  
128    from the renal vessels since the bulk of renal nerve fibers travel through the adventitia of the  
129    renal artery and the perivascular tissue to the renal hilus (28, 36, 37, 42). The wound was  
130    closed in layers and following surgery the animals were allowed to recover in the vivarium,

131 where they were kept under observation over several hours. They were given buprenorphine  
132 (0.05 mg/kg, s.c.) for analgesia peri-operatively, and as necessary following surgery.

133 For determination of renal tissue transmitter content of CGRP and norepinephrine, 24  
134 additional rats underwent unilateral renal denervation scheduled as above. However, in 12 rats  
135 surgical denervation was combined with the topical application of phenol (10% in ethanol).

136

137 Perfusion fixation: Twelve, 4 and 1 week after denervation, rats were anesthetized  
138 (methohexital, 40mg/kg i.p., + buprenorphine 0,05 mg/kg, s.c.) and the kidneys were perfused  
139 via the abdominal aorta,. Briefly, the abdominal cavity was opened and the abdominal aorta  
140 was cannulated. The inferior caval vein was cut, after which heparinized saline (150 ml NaCl  
141 0.9% + heparin 1000 IE) was infused into the aorta at a rate of 25 ml/min. Saline perfusion  
142 was followed by 350 ml of fixation solution (1% paraformaldehyde + 0.8% picric acid [pH  
143 7.2 – 7.4]) at the same rate. Both kidneys were removed and rinsed in phosphate buffer for  
144 24h, and then transferred to a 15% sucrose-phosphate buffer before they were frozen and  
145 stored at -20°C in Tissue Tek® OCT Compound (4583; Sakura-Finotech, Germany).

146

147 Immunohistochemistry: Sympathetic and sensory-peptidergic structures as well as vascular  
148 structures were labeled in the renal tissue with antibodies targeting tyrosine hydroxylase (TH;  
149 *sheep anti-TH*, 1:2000, NB 300-110, Novus Biologicals, Cambridge, UK), calcitonin gene-  
150 related peptide (CGRP; *rabbit anti-CGRP* antibody, 1:1000, T-4032, Peninsula Laboratories,  
151 San Carlos, CA), and smooth muscle actin (SMA; *mouse anti-SMA*, 1:2500, A2547, SIGMA,  
152 Saint Louis, MO, USA) (4, 47). Briefly, perfusion-fixed kidneys were cut with a cryostat (50  
153 µm) and incubated with primary antibodies diluted in Tris-buffered saline (TBS 0.05M) with  
154 1% BSA, 0.5% Triton X 100 for 24h followed by incubation with appropriate fluorochrome-  
155 tagged secondary antibodies for 1h (Alexa Flour® 488 *donkey anti-sheep* IgG, 1:1000, A-  
156 11015; Alexa Flour® 555 *donkey anti-rabbit* IgG, 1:1500, A-31572; Alexa Flour® 647

157 *donkey anti-mouse* IgG, A31571; Invitrogen Corporation, Carlsbad, CA). Staining of TH and  
158 SMA was performed simultaneously, while CGRP-staining was performed subsequently in  
159 the same samples to optimize triple-labeling. Negative control tissue was similarly treated  
160 except that primary antibodies were omitted from the first incubation step. The specificity  
161 (**Figure 1**) of the primary antibodies and the lack of interaction was established previously by  
162 pre-adsorption and pre-incubation with the respective antigens in separate experiments.

163 Sections were examined with a Nikon Eclipse E1000M microscope, equipped with a confocal  
164 system (Nikon Digital Eclipse C1). A 488nm Argon laser, a 543nm Helium-Neon Laser  
165 (Melles Griot, Carlsbad, CA), and a 638nm Diode Laser (Coherent, Santa Clara, CA) were  
166 used for excitation of Alexa 488, 555, and 647 respectively, resulting in green [TH], red  
167 [CGRP], and blue [SMA] fluorescence of the labeled structures. Unless otherwise stated, for  
168 laser-scanning of images, a Nikon 20x 0.75 microscope lens was used, resolution was set to  
169 1024 x 1024 pixel resulting in a sample area of 635 x 635  $\mu\text{m}$ . Z-axis steps were set to 0.5  $\mu\text{m}$ .

170 Since afferent and efferent nerve fibers are only sparsely and randomly dispersed in the renal  
171 interstitium we focused on the perivascular innervation, where renal nerve fibers are found in  
172 larger bundles. Representative images were taken from the entire cross-sections, but  
173 emphasis was placed on the cortical and cortico-medullary zone. Images were taken from  
174 areas with best label and the least artifact. Crystalline condensation and formation of wrinkles  
175 were the most common problems. We focused on small, representative and homogenous areas  
176 of interest within the sections instead of whole cross-sections. The area of interest was chosen  
177 visually and subjectively by a skilled examiner since automated randomizing algorithms could  
178 potentially provide inaccurate data.

179 The anatomical classification of each vessel in the area of interest was based on anatomical  
180 map within whole kidney cross-sections and by the diameter of the vessel. For the illustrative  
181 figures, single and double channel or merged three channel confocal images were adjusted for  
182 contrast and brightness using FIJI Image J (38) and Photoshop CS5.

183 In order to more easily correlate vessel size and type, e.g., interlobar, arcuate, interlobular  
184 arteries, RECA-1 antibodies (MCA970R *mouse anti-rat*; AbD Serotec, Germany) were used  
185 to label endothelial cells (12, 45) in separate adjacent sections. Panorama stacks of multiple  
186 images (4x optical magnification) were generated with a KEYENCE BZ-9000 digital  
187 microscope (Keyence, Germany).

188

189 Image analysis: In a preliminary qualitative approach, an estimation of nerve density was  
190 performed visually in 183 image stacks by 4 investigators blinded to the denervation status  
191 and time point. Tyrosine hydroxylase and CGRP label was scored in each stack (0 = none; 1 =  
192 weak; 2 = strong; 3 = very strong). Label was assessed from single channel images (*see*  
193 *Figure 2*).

194

195 FIJI Image J 1.48e was used for morphometric analysis (38). Z-projections of maximum pixel  
196 intensity were made which yielded a two-dimensional image (1024 x 1024 pixel, i.e., 635  
197 x635µm) in which each *XY*-pixel coordinate was represented by that pixel of all *Z*-steps that  
198 had the highest intensity. This image was converted into a composite file of the three color  
199 channels which allowed for splitting of the three color channels for thresholding and to  
200 remove artifacts if necessary. To approach optical *intensity* a brightness threshold was applied  
201 based on exposure values and the resulting histograms for each color channel, which yielded a  
202 binary information (i.e, positive or negative). Artifacts were removed using the region of  
203 interest (ROI) function. The resulting positive pixels were counted for each color channel  
204 (green = TH; red = CGRP; blue = SMA). Positive TH- and CGRP-labels were normalized to  
205 vascular areas (SMA). Label-*density* per region of interest (RIO) was determined by  
206 normalizing the TH or CGRP label to the area of the image or the vascular area (TH/SMA,  
207 CGRP/SMA). Non-dimensional ratios are a reasonable approach although the affinity-related  
208 staining results might vary between the respective primary and secondary antibodies.



209 Determination of tissue CGRP content: Twenty-four rats were subjected to the same unilateral  
210 surgical denervation procedure as described above. Half the rats were treated with topical  
211 application of phenol during denervation and the other half were denervated without phenol.  
212 After 12, 4 and 1 week, rats were anesthetized (methohexital, 40mg/kg i.p., + buprenorphine  
213 0,05 mg/kg, s.c.) and the kidneys were removed and divided in half and weighed. For  
214 determination of tissue CGRP content, tissue was placed in 1 ml of acetic acid (2 M) at 95°C  
215 for 10 min, homogenized (Ultra-Turrax, IKA, Staufen, Germany) and further incubated for 10  
216 min at 95°C in a preheated water bath. The suspension was centrifuged for 30 min at 10.000 g  
217 and 100 µl of the supernatant was mixed with 35 µl 5-fold concentrated enzyme-immuno  
218 assay buffer. The pH was adjusted to 7.0–7.4 with 46 µl sodium hydroxide (3 M) and CGRP  
219 was detected by ELISA (SPIbio, Bertin Pharma, France, detection limit of 5 pg/ml) (2, 20). To  
220 verify specificity of the ELISA, CGRP levels were compared in kidneys from three  $\alpha$ CGRP  
221 knockout mice and three C57Bl/6 littermates. CGRP values were  $18.2 \pm 0.7$  ng/g and  $2.5 \pm 0.3$   
222 ng/g for a wildtype and knockout mouse respectively. Non-specific binding was determined as  
223 the percent difference from wildtype (i.e., 14%). All values were corrected by 14% and  
224 expressed as ng/g wet weight.

225

226 Determination of tissue norepinephrine content: Tissue was homogenized using an Ultra-  
227 Turrax and sonicated with a micro-tipped sonifier (Sonoplus HD70, Bandelin electronic,  
228 Berlin, Germany) for 10 seconds, twice in 1M HClO<sub>4</sub> (2ml for 500mg tissue), then centrifuged  
229 at 14.000g (4°C). The catecholamines were then extracted from the supernatant using  
230 aluminum oxide adsorption. Norepinephrine (NE), epinephrine (E) and dopamine (DA) were  
231 separated and quantified using Ultraperformance Liquid Chromatography-Tandem Mass  
232 Spectrometry (UPLC-MS/MS) (13). Catecholamine content was expressed as pmol/mg wet  
233 weight.

234

235 Afferent neuronal tracing: Unilateral tracing of afferent renal nerves was performed in 4 rats  
236 as previously described (11). Briefly, rats were anesthetized as described above for the renal  
237 denervation procedure, and the dicarbocyanine dye DiI ( $\Delta^9$ -DiI, 50 mg/ml in DMSO;  
238 Molecular Probes, Eugene, OR) was applied to the subcapsular space of either the left or right  
239 kidney. Rats were allowed to recover for 1 week to permit retrograde transport of the tracer to  
240 cell bodies in dorsal root ganglia T11-L2. The ganglia were excised bilaterally and focus-  
241 stacked with a fluorescent microscope (Keyence BZ-9000). Immediately thereafter, the right  
242 and left DRGs were dissociated with collagenase (1 mg/ml), trypsin (1 mg/ml), and DNase  
243 (0.1 mg/ml). The cells were resuspended in modified L-15 medium that contained 5% rat  
244 serum, 2% chick embryo extract as well as necessary inorganic salts, amino acids, and  
245 vitamins for 1 h at 37°C (Sigma- Aldrich, Munich, Germany). Enzymatic activity was  
246 terminated by the addition of soybean trypsin inhibitor (2 mg/ml), bovine serum albumin (1  
247 mg/ml), and  $\text{CaCl}_2$  (3 mmol/l). The ganglia were triturated using sterile siliconized Pasteur  
248 pipettes to dissociate individual cells. After centrifugation, the cells were resuspended in the  
249 modified L-15 medium and plated on poly-L-lysine-coated glass. Fluorescently labeled DRG  
250 cells were counted in all samples.

251

252 Statistics: All image data were tested for normality using the Kolmogorov-Smirnov-test. Non-  
253 parametric tests were used when data failed normality testing. Analyses of observation groups  
254 (R1, L1, R4, L4, R12, L12) are herein after referred to as “*pooled observations*”. Effects of  
255 *Side* i.e. denervated vs. non-denervated *within Time* (weeks 1, 4, or 12) were determined by  
256 Mann-Whitney Rank Sum test. Effects of *Time within Side* were determined by Kruskal-  
257 Wallis One-Way ANOVA on Ranks (1W-ANOVA-oR) with Tukey and Student-Newman-  
258 Keuls post-hoc test. Finally, effects of *Side and Time* were analyzed by a Two-Way-ANOVA  
259 after rank-transformation (2W-ANOVA-aRT) (7, 14). Post-hoc pairwise multiple comparisons  
260 were performed using the Holm-Sidak method.

261 When the image stacks from individual kidneys were averaged to compare groups of rats  
262 (herein after referred to as “*averaged observations*”), the data showed a normal distribution.  
263 Analysis was performed as above, however, the appropriate parametric tests were used.  
264 Effects of *Side within Time* were analyzed by t-test. Effects of *Time within Side* were analyzed  
265 by One-Way ANOVA (1W-ANOVA) with Tukey and Student-Newman-Keuls post-hoc test.  
266 Effects of *Side and Time* were analyzed by Two-Way ANOVA (2W-ANOVA). All pairwise  
267 comparisons were performed using the Holm-Sidak method. Tissue transmitter content data  
268 showed a normal distribution and were analyzed in the same manner. Statistical significance  
269 was defined as  $P < 0.05$  (two-tailed). Results are presented either as mean $\pm$ SEM (bar plots  
270 with error bars) or as medians [1<sup>st</sup>–3<sup>rd</sup> quartile] (box-whisker plots) according to their  
271 distribution. For sake of clarity, medians in box-whisker plots are shown as vertical bars. The  
272 box boundaries denote the 1<sup>st</sup> and 3<sup>rd</sup> quartiles, whiskers indicate the 90<sup>th</sup> and 10<sup>th</sup> percentiles,  
273 small crosses indicate outliers. “R” denotes the right non-denervated kidney, “L” denotes the  
274 left denervated kidney. The numerals 1, 4, and 12 indicate the weeks after the denervation  
275 procedure when the tissue was harvested from respective groups of rats.

276

## 277 **Results**

278 All rats recovered from the renal denervation procedure and gained weight during the  
279 observation period (**Table 1**). Kidney weights also increased over time. No statistical  
280 difference could be detected between the groups of rats that were used for the different  
281 experiments, i.e. immunohistology or transmitter content measurements with or without  
282 phenol.

283

284 A total of 183 image stacks containing 702 vessel cross-sections were included in the  
285 analyses. Each stack contained 2 to 7 vessel cross-sections ranging from 8 to 665  $\mu$ m in  
286 diameter. The frequency distribution of vessel diameters did not differ significantly between

the observation groups (**Figure 3, Table 2**). Furthermore, the vessel area indicated by the area of SMA label was similar between groups (data not shown).

In nine RECA-1 labeled kidney cross-sections randomly selected from all three time points, 193 circumferential vessel cross-sections were measured. *Interlobar* artery diameters ranged from 298 to 816 $\mu$ m (median 470 $\mu$ m [425-661]; mean 526 $\mu$ m; n=22). *Arcuate* artery diameters ranged from 102 to 304 $\mu$ m (median 165 $\mu$ m [148-192]; mean 176 $\mu$ m; n=52), and *interlobular* artery diameters ranged from 40 to 162 $\mu$ m (median 85 $\mu$ m [72-103], mean 88 $\mu$ m, n=119). Brackets denote 1-3<sup>rd</sup> quartile. As shown in **Figure 3**, approximately 95% of the vessels had a diameter of less than 300 $\mu$ m, 90% less than 160 $\mu$ m and 64% less than 40 $\mu$ m. Thus, most of the observed vessels were likely downstream of interlobular and arcuate arteries, and only 5% were large vessels in the range of interlobar arteries.

### **Visual analysis**

Qualitative visual analysis demonstrated decreased TH- and CGRP-positive label one week after denervation (L1\_TH<sup>score</sup> 1.33[1.00-2.00] vs. R1\_TH<sup>score</sup> 2.33 [2.00-3.00],  $P<0.05$ ; L1\_CGRP<sup>score</sup> 0.67 [0.00-1.33] vs. R1\_CGRP<sup>score</sup> 2.33 [1.08-2.67],  $P<0.05$ ), which appeared to completely recover by week 12 (L12\_TH<sup>score</sup> 2.33 [1.67-3.00] vs. R12\_TH<sup>score</sup> 2.67 [2.33-3.00],  $P=ns$ ; L12\_CGRP<sup>score</sup> 2.00 [1.33-2.67] vs. R12\_CGRP<sup>score</sup> 2.33 [1.67-2.67],  $P=ns$ ). Representative micrographs are shown in **Figure 4 and 5**.

### **Morphometric analysis (TH)**

Results of the morphometric analysis of TH<sup>+</sup> staining in “pooled observations” are shown in **Figure 6**. Decreased TH<sup>+</sup> pixel counts were found on the denervated side, one week after surgery. TH<sup>+</sup> label on the denervated side had recovered to R1\_TH levels by 4 weeks and remained there at 12 weeks post surgery. However, at 12 weeks, TH<sup>+</sup> pixel counts on the denervated side remained lower than the non-denervated side.

313 The analyses based on “*averaged observations*” similarly showed reduced TH<sup>+</sup> pixel counts  
 314 (given as *absolute pixel count/sample area*, i.e. 1024x1024 pixels) one week after surgery in  
 315 denervated kidneys compared to non-denervated kidneys (R1\_TH: 2886 ± 482 vs. L1\_TH:  
 316 374 ± 109; *P* = 0.019; 2W-ANOVA). By week 4 and 12 weeks, the TH<sup>+</sup> pixel-counts in  
 317 denervated kidneys reached the R1\_TH level (R1\_TH vs. L4\_TH: 3093 ± 498 and L12\_TH:  
 318 4437 ± 1613; *P* = 0.562; 2W-ANOVA). The non-denervated kidneys showed increased TH<sup>+</sup>  
 319 pixel-counts 4 and 12 weeks after denervation (R1\_TH vs. R4\_TH: 7866 ± 1383 and  
 320 R12\_TH: 6725 ± 1693; *P* < 0.027; 2W-ANOVA, 1W-ANOVA). However, the denervated  
 321 TH<sup>+</sup> pixel-counts at week 12 tended to be lower than the non-denervated side, but no statistical  
 322 difference between right and left kidneys was observed in week 12 (R12\_TH vs. L12\_TH; *P* =  
 323 0.175; 2W-ANOVA).

324

#### 325 Morphometric analysis (CGRP)

326 The analysis of CGRP<sup>+</sup> pixel counts based on “*pooled observations*” is shown in **Figure 7**.  
 327 Briefly, a significant decrease in CGRP<sup>+</sup> label was observed on the denervated side, which  
 328 recovered to the R1\_CGRP levels within 4 weeks. Furthermore, an increase on the non-  
 329 denervated side was also observed. However, no statistical difference was detected between  
 330 the non-denervated and the denervated side in week 12.

331

332 The CGRP<sup>+</sup> staining based on “*averaged observations*” in week 1 similarly showed decreased  
 333 CGRP<sup>+</sup> pixel counts in the denervated kidneys compared to the non-denervated kidneys  
 334 (R1\_CGRP: 766 ± 149 vs. L1\_CGRP: 43 ± 12; *P*=0.024; 2W-ANOVA). By week 4 and 12,  
 335 the CGRP<sup>+</sup> pixel-counts in the denervated kidneys reached and tended to surpass the  
 336 R1\_CGRP level (R1\_CGRP vs. L4\_CGRP: 718 ± 137 and L12\_CGRP: 1638 ± 520; *P* ≥  
 337 0.271; 2W-ANOVA, 1W-ANOVA). The non-denervated kidneys showed increased CGRP<sup>+</sup>  
 338 pixel-counts in weeks 4 and 12 (R1\_CGRP vs. R4\_CGRP: 2174 ± 437 and R12\_CGRP: 1874

339  $\pm 417$ ;  $P < 0.027$ ; 2W-ANOVA, 1W-ANOVA). No differences in CGRP<sup>+</sup> pixel-counts were  
340 observed between right and left kidneys in week 12 (R12\_CGRP vs. L12\_CGRP;  $P = 0.627$ ;  
341 2W-ANOVA).

342

#### 343 Morphometric analysis (TH/SMA)

344 For “pooled observations” we found decreased TH/SMA on the denervated side one week  
345 after denervation (R1\_TH/SMA: 0.071 [0.037-0.141] vs. L1\_TH/SMA: 0.007 [0.002-0.014];  
346  $P < 0.0001$ ; 2W-ANOVA-aRT), which recovered to R1\_TH/SMA levels by week 4 and  
347 remained there at 12 weeks (L4\_TH/SMA: 0.052 [0.042-0.083]; L12\_TH/SMA: 0.106  
348 [0.0794-0.153];  $P = 0.253$ ; 2W-ANOVA-aRT, 1W-ANOVA-oR). The TH/SMA on the  
349 denervated side at weeks 4 and 12 (L4\_TH/SMA and L12\_TH/SMA) were lower than that on  
350 the non-denervated side (R4\_TH/SMA: 0.147 [0.100-0.246]; R12\_TH/SMA: 0.159 [0.094-  
351 0.206];  $P = 0.024$ ; 2W-ANOVA-aRT). An increase in TH/SMA on the non-denervated side  
352 was observed (R1\_CGRP vs. R4\_CGRP & R12\_CGRP;  $P < 0.001$ ; 1W-ANOVA-oR).

353

354 The “averaged observations” analysis yielded similar results, which are displayed in **Figure 8**.  
355 Briefly, a significant decrease in TH/SMA was found one week after denervation, which  
356 recovered to R1\_TH/SMA levels within 4 to 12 weeks. At 12 weeks the TH/SMA ratio on the  
357 denervated side tended to be lower than on the non-denervated side.

358

#### 359 Morphometric analysis (CGRP/SMA)

360 Based on “pooled observations” a decrease in the CGRP/SMA ratio was found one week  
361 after denervation (R1\_CGRP/SMA: 0.019 [0.007-0.051] vs. L1\_CGRP/SMA: 0.00062  
362 [0.00006-0.00187];  $P < 0.0001$ ; 2W-ANOVA-aRT) which recovered to the R1\_CGRP/SMA  
363 level by week 4 (L4\_CGRP/SMA: 0.0140 [0.0082-0.262];  $P = 0.411$ ; 2W-ANOVA-aRT) and  
364 even surpassed the R1\_CGRP/SMA level by week 12 (L12\_CGRP/SMA: 0.039 [0.028-

0.055];  $P = 0.024$ ; 2W-ANOVA-aRT, 1W-ANOVA-oR). The CGRP/SMA on the denervated side in week 4 (L4\_CGRP/SMA) was lower than on the non-denervated side (R4\_CGRP/SMA: 0.045 [0.029-0.054];  $P < 0.0001$ ; 2W-ANOVA-aRT) but was no longer different from the non-denervated side by week 12 (R12\_CGRP/SMA: 0.0455 [0.0305-0.0670];  $P = 0.255$ ; 2W-ANOVA-aRT). There was an increase in CGRP/SMA on the non-denervated side (R1\_CGRP vs. R4\_CGRP and R12\_CGRP;  $P = 0.007$ ; 1W-ANOVA-oR).

371

The analysis based on “*averaged observations*” for the CGRP/SMA yielded similar results (**Figure 9**). One week after denervation a significant decrease of CGRP/SMA was found which recovered to the R1\_CGRP/SMA level by week 4 and surpassed the R1\_CGRP/SMA level by week 12. The CGRP/SMA on the denervated side in week 4 (L4\_CGRP/SMA) was lower than on the non-denervated side in week 4, but no longer different from the non-denervated side in week 12. Furthermore, there was an increase of CGRP/SMA on the non-denervated side at week 4 and 12.

379

#### 380 Morphometric analysis (CGRP/TH)

Based on “pooled observations” the CGRP/TH of the denervated kidneys was shifted towards CGRP-positive label (L1\_CGRP/TH: 0.147 [0.0527-0.440] vs. L4\_CGRP/TH 0.219 [0.103-0.542] vs. L12\_CGRP/TH: 0.402 [0.280-0.528];  $P = 0.019$ ; 1W-ANOVA-oR). No such shift was observed on the non-denervated side (R1\_CGRP/TH 0.276 [0.0856-0.462] vs. R4\_CGRP/TH 0.309 [0.171-0.392] vs. R12\_CGRP/TH 0.318 [0.256-0.463];  $P = 0.194$ ; 1W-ANOVA-oR). Based on “*averaged observations*” the results were similar (**Figure 10**).

387

388 Tissue transmitter content

389 Tissue analysis revealed a decrease of CGRP content by approximately 72% one week after  
390 surgery in denervated kidneys compared to non-denervated kidneys. By week 12, the CGRP  
391 content in denervated kidneys was no longer significantly different from innervated kidneys.  
392 A decrease in NE of approximately 78% was found in denervated kidneys 1 week after  
393 surgery. Norepinephrine values in the denervated kidneys remained lower throughout the 12  
394 week study. No significant levels of epinephrine or dopamine were detected. The addition of  
395 phenol to the denervation procedure did not significantly influence tissue levels of NE or  
396 CGRP (*Figure 11 and 12*).

397

398 Afferent neuronal tracing

399 No evidence of contralateral labeling by DiI was identified in either whole ganglia or in  
400 cultured DRG cells. In accordance with previous studies (11), cell cultures from the ipsilateral  
401 side showed that  $14 \pm 1\%$  of cells were labeled by DiI.

402

403 **Discussion**

404 Here, we investigated the re-innervation of afferent peptidergic and efferent sympathetic  
405 nerves in a rat model of unilateral surgical renal denervation. Based on a purely morphological  
406 analysis, we found strong evidence that the denervation procedure in male Sprague-Dawley  
407 rats decreased both efferent and the afferent innervation of small renal vessels within one  
408 week of surgery indicating subtotal denervation, and that both regrew within 4 weeks of  
409 denervation. Furthermore, by 12 weeks after denervation, we found evidence that TH  
410 immunoreactivity surrounding small vessels of the intact kidney was greater than that  
411 observed 1 week after surgery, suggesting that the area of the vessel covered by neural tissue  
412 increased in the intact kidney as a consequence of denervation of the contralateral kidney. A  
413 similar outcome was found for CGRP immunoreactivity suggesting that both sympathetic and



414 sensory afferents are influenced by denervation in a parallel manner. Furthermore, within 12  
415 weeks CGRP immunoreactivity of the denervated kidney surpassed the basal level of the  
416 intact kidney, indicating overshooting afferent innervation.

417 Interestingly, data comparing TH and CGRP area suggest that CGRP regrowth outpaced that  
418 of the sympathetic nerves. This latter interpretation was confirmed by assessments of tissue  
419 neurotransmitter content, which showed deficits in NE throughout the post-surgical  
420 assessment period, while CGRP content had recovered by 12 weeks post denervation.

421 The immunostaining approach used here for determination of nerve regrowth is limited in that  
422 it does not provide information about the structure or function of new nerve fibers. It is not  
423 possible, for instance, to determine whether the increase in immunoreactivity is due to a  
424 greater density of axons or dendrites, a higher degree of branching of the regrown axons, or an  
425 increased number of varicosities containing the respective labeled antigens. However,  
426 constrictive nerve injury has been shown to increase the density of peptidergic and  
427 sympathetic fibers, possibly through migration and branching of sprouting nerve fibers (49).

428 Our evidence that NE and CGRP content in the intact kidney did not increase overtime  
429 seemingly contradicts our histological evidence of hyperinnervation of the intact kidney by  
430 both the sensory afferent and sympathetic efferent systems and the overshooting re-  
431 innervation of the denervated kidney by sensory afferent nerves. Though both the NE and  
432 CGRP content were reduced to a similar extent in the denervated kidney, only CGRP  
433 concentrations appeared to return to levels close to baseline. These findings also seem to  
434 contradict our morphological evidence of re-innervation of denervated kidney by sympathetic  
435 efferents. Our findings are instead consistent with immunohistochemical evidence reported by  
436 others which showed that the neuronal marker PGP9.5 returned to baseline levels within 6  
437 months of syngeneic rat renal transplantation indicating re-innervation, while NE content in the  
438 transplanted kidney remained low until 9 months after transplant (23). Although reliable  
439 functional conclusions cannot be drawn from these findings, it seems that the sympathetic

440 efferent re-innervation is functionally inadequate.

441 It is not clear why neurotransmitter content was not increased in the non-denervated kidney  
442 despite histological evidence of hyperinnervation, a finding that was more robust for the  
443 afferent nerves. It is possible that an apparent hyperinnervation in intact kidneys was due to  
444 the continued maturation and growth of the sympathetic and sensory innervation of the kidney  
445 between weeks 1 and 12 post denervation. However, a previous report indicates that in  
446 normotensive rats, the distribution of sympathetic and sensory innervation of the kidney is  
447 similar to the adult by 21 days of age (31). Nevertheless, we cannot rule out maturation as a  
448 cause for increased area of innervation in the non-denervated kidneys at 12 weeks due to the  
449 lack of an untreated time-matched control group.

450 Indeed, our histological methods are limited by our inability to obtain measures of TH and  
451 CGRP intensity throughout the full thickness of the vessel, as only surface areas could be  
452 appropriately imaged. Furthermore, we utilized thresholding and Z-projection to compress  
453 volume information to a two dimensional area. Using this method we are limited to the  
454 determination of a 2 dimensional area of visible vessels covered by immunoreactive  
455 components of the nerve. Because we used a thresholding method, we are only describing the  
456 area of TH expression, rather than the intensity of expression. Moreover, our antibody  
457 detected total TH rather than phosphorylated forms of the enzyme so we were unable to  
458 measure indices of TH activity in regrown nerves. We cannot make inferences about the level  
459 of TH expression or its activity and certainly not norepinephrine content. Thus, a clear-cut  
460 correlation between NE tissue content and TH-positive label cannot be expected.

461 In contrast, CGRP tissue content would more likely correlate with the cumulative fiber  
462 volume of sensory nerves because sensory neuro-peptides such as CGRP are stored and  
463 secreted along the length of the axon (10, 25, 46). Nevertheless, the label observed using our  
464 methods is related only to the diameter of the vessel given that thresholding and Z-projection  
465 reduces the measurement to a 2 dimensional area. The volume of the nerve cannot be

determined. Given that the fibers are more or less cylindrical in shape, changes in diameter will lead to quadratic changes of volume. Thus, many small fibers, which represent the same surface information as a single large fiber will contain far less transmitter than the single large fiber. Therefore, sprouting of very small and highly branched nerve fibers (49) will not necessarily be associated with an increased tissue transmitter content. Predicting the influence of denervation on NE neurotransmission using 2 dimensional TH immunolabel is further complicated by the fact that NE production is presumably amplified from the amount of TH through the enzymatic cascade, whereas CGRP label provides a more direct indication of the amount of neurotransmitter present.

An additional complication lies in the fact that we chose areas for image analysis based on consistent and reliable labeling, whereas the NE and CGRP content represent neurotransmitter available in the whole kidney. It is possible that the discrepancy lies in the fact that we examined areas with the most robust label. It is possible that regrowth had not yet reached areas where reliable label was more difficult to obtain. Though we cannot conclude with certainty that an apparent increase in innervation of the intact kidney was dependent on the denervation procedure due to the lack of time control experiments, it is clear that peptidergic reinnervation of the denervated kidney dominated sympathetic reinnervation. No such dominance in peptidergic growth was found on the non-denervated kidneys. These latter findings are in accordance with our tissue measurements.

Functional interpretations of our findings remain speculative. Though there is evidence for both inhibitory (8, 10, 44) and excitatory effects (3, 21) of renal peptidergic afferent innervation, it is tempting to suggest that a net surplus of afferent activity could contribute to an overall decrease in sympathetic activity (10). In patients, we noted that renal denervation did not affect renal vascular resistance or perfusion, but did lower indices of systemic vascular resistance (35). Renal haemodynamics have been shown to be relatively free from the influence of the renal sympathetic nerves. However, this is might be more apparent than real

492 as the renal vasculature has powerful autoregulatory mechanisms that come into play, perhaps  
493 offsetting the vasoconstrictor action of the renal sympathetic nerves (15, 16, 24). Interestingly,  
494 sensory afferents have been reported to play key role in myogenic contraction of blood vessels  
495 and thus in autoregulation (41). In a separate study, renal denervation in hypertensive patients  
496 was found to lower blood pressure and muscle sympathetic nerve activity (MSNA), as well as  
497 whole body catecholamine spill-over (39). Moreover, the hypotensive effects appeared to be  
498 long-lasting (17).

499 An additional limitation of the study was our focus on the intrarenal vasculature in the  
500 periphery of the kidney downstream of interlobular and arcuate arteries, rather than the  
501 interstitial tissue, the latter of which might have a more significant impact on the hypotensive  
502 effects of denervation. The innervation of the interstitium is not homogenous, but is instead  
503 patchy and focally distributed. Thus, morphometric analysis of interstitial innervation is much  
504 more difficult to standardize. Here we focused on the perivascular nerves due to our recent  
505 finding that stimulation of intrarenal afferents by injection of the TRPV1 receptor agonist  
506 capsaicin into the renal artery, resulted in a tonic inhibition of contralateral renal sympathetic  
507 nerve activity (10). Though the renal parenchyma is far less densely innervated than the renal  
508 pelvis, there exists a reasonable density of intrarenal innervation in the perivascular and  
509 adventitial space. The density of the afferent peptidergic fibers is far less than that of the  
510 sympathetic nerves even around the vessels. In the study by Mulder et al., intrarenal afferents  
511 were not even mentioned (34). We found the ratio of afferent-to-efferent fiber density ranged  
512 from 0.15 to 0.4 in the non-denervated kidney which is in accordance with recently published  
513 data (33). This ratio was shifted towards sensory innervation on the denervated side. Such a  
514 shift has not yet been described. It is not yet clear if this complex reinnervation pattern  
515 identified in intrarenal perivascular nerves also occurs in the renal pelvic nerves, because our  
516 study exclusively focused intrarenal innervation and recent studies did not investigate this  
517 question (6, 34).

518 The thermophysical endovascular denervation procedure used for human hypertension therapy  
519 exerts its main effects in the perivascular space (36, 37, 42). Though our unilateral subtotal  
520 denervation model does not perfectly simulate the clinical procedures, our approach does  
521 provide new insight into renal reninnervation processes.

522 Our morphological findings support the work recently published by Mulder et al., which  
523 showed a complete regrowth of the renal pelvic afferent and intrarenal efferent innervation  
524 twelve weeks after unilateral renal denervation (34). In their work, the renal denervation  
525 procedure included the use of phenol application to the surface of the vasculature after  
526 surgical stripping of the adventitia. Our work extends these findings by describing intrarenal  
527 afferent and efferent innervation without the use of phenol. We purposely omitted the use  
528 phenol for the denervation procedure in order to investigate patterns of reinnervation after  
529 subtotal denervation in an effort to better mimic the subtotal denervation achieved in clinical  
530 renal denervation procedures. Our evidence suggests that the use of phenol does not have  
531 much effect on re-innervation properties, as both CGRP and NE content in the denervated  
532 kidney were similar whether denervation included phenol or not. Furthermore, we could not  
533 detect any intramural nerves in the renal artery that would definitely require the use of phenol  
534 (Figure 1).

535 To our knowledge this is the first study, which indicates a contralateral effect of unilateral  
536 denervation of the kidney. We ruled out the possibility of bilateral innervation of the kidney  
537 from the same source. Our neuronal tracing experiments failed to identify any monosynaptic  
538 innervation from the kidney to the contralateral dorsal root ganglia in the healthy rat. The  
539 exact mechanisms for altered contralateral innervation are not clear. The release of humoral  
540 factors at the lesion site or some communication to the contralateral side by neuronal  
541 mechanisms are speculated to play a role (27). A recent study in sheep reported complete  
542 morphological and functional re-innervation the latter of which was tested by electrical  
543 stimulation. However, in this study no interaction between the denervated and un-denervated

544 kidney was described and no distinction was made between intrarenal and pelvic re-  
545 innervation.

546 Finally, even the source of reinnervation is not completely clear. It has been reported that the  
547 removal of postganglionic cell bodies by celiac ganglionectomy could not permanently ablate  
548 sympathetic innervation of splanchnic organs. In fact, sympathetic fibers innervating the  
549 kidney demonstrated the most prominent regrowth after ganglionectomy in rats (29, 48). After  
550 cell body removal (ganglionectomy), sympathetic re-innervation must occur via sprouting  
551 from other ganglia. After axotomy (as was done here), it is not quite clear whether the source  
552 of re-innervation is from the same ganglia, or via sprouting from other sources, or both.

553

554 ***Perspective:***

555 Although the functional significance of our indirect measures of re-innervation has yet to be  
556 defined, our data provide important insight into the complexity of the renal re-innervation  
557 process. A complex re-innervation pattern with a shift towards afferent innervation seems to  
558 take place. Our study provides the framework for well-designed in-vivo studies that are  
559 necessary to further substantiate our understanding of renal innervation and its function in  
560 health and disease. Since renal re-innervation seems to be a multi-species phenomenon it must  
561 also be expected in humans over months after percutaneous renal denervation. Long-term  
562 effects on blood pressure and sympathetic control described in humans might rather be due to  
563 a regenerative remodeling of renal nerves than complete and long lasting loss of innervation.

564

565    **Acknowledgment:**

566    none

567

568    **Sources of Funding:**

569    SFB 423, Deutsche Forschungsgemeinschaft; MEDTRONIC

570

571    **Conflict(s) of interest/Disclosure:**

572    RV and TD received funding from MEDTRONIC

573

- 575 1. Catheter-based renal sympathetic denervation for resistant hypertension: durability of  
576 blood pressure reduction out to 24 months. *Hypertension* 57: 911-917, 2011.
- 577 2. **Averbeck B, and Reeh PW.** Interactions of inflammatory mediators stimulating  
578 release of calcitonin gene-related peptide, substance P and prostaglandin E(2) from isolated rat  
579 skin. *Neuropharmacology* 40: 416-423, 2001.
- 580 3. **Barry EF, and Johns EJ.** Intrarenal bradykinin elicits reno-renal reflex sympatho-  
581 excitation and renal nerve-dependent fluid retention. *Acta Physiol (Oxf)* 213: 731-739, 2015.
- 582 4. **Bergua A, SchrodL F, and Neuhuber WL.** Vasoactive intestinal and calcitonin gene-  
583 related peptides, tyrosine hydroxylase and nitrergic markers in the innervation of the rat  
584 central retinal artery. *Exp Eye Res* 77: 367-374, 2003.
- 585 5. **Bhatt DL, Kandzari DE, O'Neill WW, D'Agostino R, Flack JM, Katzen BT, Leon  
586 MB, Liu M, Mauri L, Negoita M, Cohen SA, Oparil S, Rocha-Singh K, Townsend RR,  
587 and Bakris GL.** A controlled trial of renal denervation for resistant hypertension. *N Engl J*  
588 *Med* 370: 1393-1401, 2014.
- 589 6. **Booth LC, Nishi EE, Yao ST, Ramchandra R, Lambert GW, Schlaich MP, and  
590 May CN.** Reinnervation of renal afferent and efferent nerves at 5.5 and 11 months after  
591 catheter-based radiofrequency renal denervation in sheep. *Hypertension* 65: 393-400, 2015.
- 592 7. **Conover WJ.** The rank transformation—an easy and intuitive way to connect many  
593 nonparametric methods to their parametric counterparts for seamless teaching introductory  
594 statistics courses. *Wiley Interdisciplinary Reviews: Computational Statistics* 4: 432-438, 2012.
- 595 8. **DiBona GF, and Esler M.** Translational medicine: the antihypertensive effect of renal  
596 denervation. *Am J Physiol Regul Integr Comp Physiol* 298: R245-253, 2010.
- 597 9. **DiBona GF, and Kopp UC.** Neural control of renal function. *Physiol Rev* 77: 75-197,  
598 1997.
- 599 10. **Ditting T, Freisinger W, Siegel K, Fiedler C, Small L, Neuhuber W, Heinlein S,  
600 Reeh PW, Schmieder RE, and Veelken R.** Tonic postganglionic sympathetic inhibition  
601 induced by afferent renal nerves? *Hypertension* 59: 467-476, 2012.
- 602 11. **Ditting T, Tiegs G, Rodionova K, Reeh PW, Neuhuber W, Freisinger W, and  
603 Veelken R.** Do distinct populations of dorsal root ganglion neurons account for the sensory  
604 peptidergic innervation of the kidney? *Am J Physiol Renal Physiol* 297: F1427-1434, 2009.
- 605 12. **Duijvestijn AM, van Goor H, Klatter F, Majoor GD, van Bussel E, and van Breda  
606 Vriesman PJ.** Antibodies defining rat endothelial cells: RECA-1, a pan-endothelial cell-  
607 specific monoclonal antibody. *Lab Invest* 66: 459-466, 1992.
- 608 13. **Dunand M, Gubian D, Stauffer M, Abid K, and Grouzmann E.** High-throughput  
609 and sensitive quantitation of plasma catecholamines by ultraperformance liquid  
610 chromatography-tandem mass spectrometry using a solid phase microwell extraction plate.  
611 *Anal Chem* 85: 3539-3544, 2013.
- 612 14. **Dytham C.** Choosing And Using Statistics: A Biologist's Guide. In: *Choosing And*  
613 *Using Statistics: A Biologist's Guide* Wiley-Blackwell, 2011, p. 160-182.
- 614 15. **Eppel GA, Denton KM, Malpas SC, and Evans RG.** Nitric oxide in responses of  
615 regional kidney perfusion to renal nerve stimulation and renal ischaemia. *Pflugers Arch* 447:  
616 205-213, 2003.
- 617 16. **Eppel GA, Lee LL, and Evans RG.** alpha-Adrenoceptor subtypes mediating regional  
618 kidney blood flow responses to renal nerve stimulation. *Auton Neurosci* 112: 15-24, 2004.
- 619 17. **Esler MD, Krum H, Schlaich M, Schmieder RE, Bohm M, and Sobotka PA.** Renal  
620 sympathetic denervation for treatment of drug-resistant hypertension: one-year results from  
621 the Symplicity HTN-2 randomized, controlled trial. *Circulation* 126: 2976-2982, 2012.



18. **Esler MD, Krum H, Sobotka PA, Schlaich MP, Schmieder RE, and Bohm M.** Renal sympathetic denervation in patients with treatment-resistant hypertension (The Symplicity HTN-2 Trial): a randomised controlled trial. *Lancet* 376: 1903-1909, 2010.
19. **Feng NH, Lee HH, Shiang JC, and Ma MC.** Transient receptor potential vanilloid type 1 channels act as mechanoreceptors and cause substance P release and sensory activation in rat kidneys. *Am J Physiol Renal Physiol* 294: F316-325, 2008.
20. **Fischer MJ, Reeh PW, and Sauer SK.** Proton-induced calcitonin gene-related peptide release from rat sciatic nerve axons, in vitro, involving TRPV1. *Eur J Neurosci* 18: 803-810, 2003.
21. **Foss JD, Wainford RD, Engeland WC, Fink GD, and Osborn JW.** A novel method of selective ablation of afferent renal nerves by periaxonal application of capsaicin. *Am J Physiol Regul Integr Comp Physiol* 308: R112-122, 2015.
22. **Gazdar AF, and Dammin GJ.** Neural degeneration and regeneration in human renal transplants. *NEnglJMed* 283: 222-224, 1970.
23. **Grisk O, Grone HJ, Rose HJ, and Rettig R.** Sympathetic reinnervation of rat kidney grafts. *Transplantation* 72: 1153-1155, 2001.
24. **Guild SJ, Eppel GA, Malpas SC, Rajapakse NW, Stewart A, and Evans RG.** Regional responsiveness of renal perfusion to activation of the renal nerves. *Am J Physiol Regul Integr Comp Physiol* 283: R1177-1186, 2002.
25. **Huang LY, and Neher E.** Ca(2+)-dependent exocytosis in the somata of dorsal root ganglion neurons. *Neuron* 17: 135-145, 1996.
26. **Koepke JP, Jones S, and DiBona GF.** Renal nerves mediate blunted natriuresis to atrial natriuretic peptide in cirrhotic rats. *American Journal of Physiology* 252: R1019-R1023, 1987.
27. **Koltzenburg M, Wall PD, and McMahon SB.** Does the right side know what the left is doing? *Trends Neurosci* 22: 122-127, 1999.
28. **Krum H, Schlaich M, Whitbourn R, Sobotka PA, Sadowski J, Bartus K, Kapelak B, Walton A, Sievert H, Thambar S, Abraham WT, and Esler M.** Catheter-based renal sympathetic denervation for resistant hypertension: a multicentre safety and proof-of-principle cohort study. *Lancet* 373: 1275-1281, 2009.
29. **Li M, Galligan J, Wang D, and Fink G.** The effects of celiac ganglionectomy on sympathetic innervation to the splanchnic organs in the rat. *Auton Neurosci* 154: 66-73, 2010.
30. **Linz D, Mahfoud F, Schotten U, Ukena C, Neuberger HR, Wirth K, and Bohm M.** Renal sympathetic denervation suppresses postapneic blood pressure rises and atrial fibrillation in a model for sleep apnea. *Hypertension* 60: 172-178, 2012.
31. **Liu L, and Barajas L.** The rat renal nerves during development. *Anat Embryol (Berl)* 188: 345-361, 1993.
32. **Mahfoud F, Schlaich M, Kindermann I, Ukena C, Cremers B, Brandt MC, Hoppe UC, Vonend O, Rump LC, Sobotka PA, Krum H, Esler M, and Bohm M.** Effect of renal sympathetic denervation on glucose metabolism in patients with resistant hypertension: a pilot study. *Circulation* 123: 1940-1946, 2011.
33. **Milosavljevic Z, Zelen I, and Sazdanovic M.** Autonomic innervation of the periglomerular arteries. *Anal Quant Cytopathol Histopathol* 36: 161-166, 2014.
34. **Mulder J, Hokfelt T, Knuepfer MM, and Kopp UC.** Renal sensory and sympathetic nerves reinnervate the kidney in a similar time-dependent fashion after renal denervation in rats. *Am J Physiol Regul Integr Comp Physiol* 304: R675-682, 2013.
35. **Ott C, Janka R, Schmid A, Titze S, Ditting T, Sobotka PA, Veelken R, Uder M, and Schmieder RE.** Vascular and renal hemodynamic changes after renal denervation. *Clin J Am Soc Nephrol* 8: 1195-1201, 2013.

36. **Roy AK, Fabre A, Cunningham M, Buckley U, Crotty T, and Keane D.** Post mortem study of the depth and circumferential location of sympathetic nerves in human renal arteries-Implications for renal denervation catheter design. *Catheter Cardiovasc Interv* 2015.
37. **Sakakura K, Ladich E, Cheng Q, Otsuka F, Yahagi K, Fowler DR, Kolodgie FD, Virmani R, and Joner M.** Anatomic assessment of sympathetic peri-arterial renal nerves in man. *J Am Coll Cardiol* 64: 635-643, 2014.
38. **Schindelin J, Arganda-Carreras I, Frise E, Kaynig V, Longair M, Pietzsch T, Preibisch S, Rueden C, Saalfeld S, Schmid B, Tinevez JY, White DJ, Hartenstein V, Eliceiri K, Tomancak P, and Cardona A.** Fiji: an open-source platform for biological-image analysis. *Nat Methods* 9: 676-682, 2012.
39. **Schlaich MP, Sobotka PA, Krum H, Lambert E, and Esler MD.** Renal sympathetic-nerve ablation for uncontrolled hypertension. *N Engl J Med* 361: 932-934, 2009.
40. **Schlaich MP, Sobotka PA, Krum H, Whitbourn R, Walton A, and Esler MD.** Renal denervation as a therapeutic approach for hypertension: novel implications for an old concept. *Hypertension* 54: 1195-1201, 2009.
41. **Scotland RS, Chauhan S, Davis C, De Felipe C, Hunt S, Kabir J, Kotsonis P, Oh U, and Ahluwalia A.** Vanilloid receptor TRPV1, sensory C-fibers, and vascular autoregulation: a novel mechanism involved in myogenic constriction. *Circ Res* 95: 1027-1034, 2004.
42. **Simionescu N SM.** The cardiovascular system. In: *Cell and tissue biology A textbook of histology*, edited by (ed) WL. Baltimore: Urban & Schwarzenberg, 1988, p. 355-400.
43. **Smithwick RH, and Thompson JE.** Splanchnicectomy for essential hypertension; results in 1,266 cases. *J Am Med Assoc* 152: 1501-1504, 1953.
44. **Stella A, and Zanchetti A.** Functional role of renal afferents. *Physiol Rev* 71: 659-682, 1991.
45. **Ulger H, Karabulut AK, and Pratten MK.** Labelling of rat endothelial cells with antibodies to vWF, RECA-1, PECAM-1, ICAM-1, OX-43 and ZO-1. *Anat Histol Embryol* 31: 31-35, 2002.
46. **Weller K, Reeh PW, and Sauer SK.** TRPV1, TRPA1, and CB1 in the isolated vagus nerve - Axonal chemosensitivity and control of neuropeptide release. *Neuropeptides* 45: 391-400, 2011.
47. **Worl J, Mayer B, and Neuhuber WL.** Spatial relationships of enteric nerve fibers to vagal motor terminals and the sarcolemma in motor endplates of the rat esophagus: a confocal laser scanning and electron-microscopic study. *Cell Tissue Res* 287: 113-118, 1997.
48. **Yamada M, Terayama R, Bando Y, Kasai S, and Yoshida S.** Regeneration of the abdominal postganglionic sympathetic system. *Neurosci Res* 54: 261-268, 2006.
49. **Yen LD, Bennett GJ, and Ribeiro-da-Silva A.** Sympathetic sprouting and changes in nociceptive sensory innervation in the glabrous skin of the rat hind paw following partial peripheral nerve injury. *J Comp Neurol* 495: 679-690, 2006.

712 **Tables**

713 **Table 1:**

Group	<i>week 1</i>	<i>week 4</i>	<i>week 12</i>	
<i>Body weight</i>	267±7g	375±6g	528±21g	<i>P</i> <0.05
<i>Kidney weight</i>	1.17±0.12g	1.32±0.08g	1.40±0.06g	<i>P</i> <0.05

714

715 Table 1 shows the mean body- and kidney weights (±SEM) of all rats in the study. Body  
 716 weight as well as kidney weight increased significantly between each observation time-point.

717

718 **Table 2:**

Weeks post surgery	n	<b>Right kidneys (<i>non-denervated</i>)</b>			<b>Left kidneys (<i>denervated</i>)</b>		
		<b>Group</b>	Image stacks (n=)	Vessels (n=)	<b>Group</b>	Image stacks (n=)	Vessels (n=)
1	4	<b><i>R1</i></b>	31	111	<b><i>L1</i></b>	53	216
4	4	<b><i>R4</i></b>	23	93	<b><i>L4</i></b>	24	94
12	4	<b><i>R12</i></b>	26	97	<b><i>L12</i></b>	26	91

719

720 Table 2 shows the observation groups of the study. Indicated are: the number of image stacks  
 721 taken from each group of kidneys and the cumulative number of vessel cross sections  
 722 contained in theses image stacks are given.

723

724 **Figure legends**

725 **Figure 1:** Vessel wall sector (Arteria renalis; 100 x 160  $\mu\text{m}$ , 100x oil immersion) with  
726 perivascular innervation. A) TH-positive nerve fibers. B) CGRP-positive nerve fibers. C)  
727 Immediate vicinity of sympathetic (TH-positive) and afferent (CGRP-positive) nerve fibers  
728 yields yellowish or light green color. No nerve fibers are visible in the vessels wall. (Scale bar  
729 = 40 $\mu\text{m}$ ).

730

731 **Figure 2:** Representative image stack (renal cortex 635 $\mu\text{m}$  x 635 $\mu\text{m}$ ) from a right non-  
732 denervated kidney (the corresponding triple-channel image is shown in *Figure 5A*). A) “green  
733 channel” stained for TH = efferent sympathetic. B) “red channel” stained for CGRP =  
734 peptidergic afferent. CGRP staining was always much weaker than TH staining (score = 3,  
735 both channels). (Scale bar = 200 $\mu\text{m}$ ).

736

737 **Figure 3:** Frequency distribution of the vessel diameters (bin-width = 10 $\mu\text{m}$ ) of 702 vessels  
738 contained in 183 image stacks from all observation groups (*see Table 1*). The striped bars in  
739 the upper part of the left panel mark the vessel diameter ranges. Black: interlobular and  
740 smaller; Gray: arcuate; White: interlobar; The frequency distribution did not differ  
741 significantly between observation groups (middle and right panels).

742

743 **Figure 4:** Representative images of large renal vessels labeled for TH- (green = sympathetic  
744 efferent), CGRP- (red = peptidergic afferent) and SMA-immunoreactivity (blue = vascular  
745 area). Yellow or light green label results from immediate vicinity of TH- and CGRP- staining.  
746 A) Right – non-denervated, week 1 [R1]; B) Left – denervated, week 1 [L1]; C) Right – non-  
747 denervated, week 12 [R12]; D) Left – denervated, week 12 [L12]. Few nerves are visible in  
748 L1. L12 looks very similar to R1 and R12. Large yellow structures show close proximity of

749 both fiber types and are major nerve trunks containing efferent and afferent fibers. (Scale bar  
750 = 200 $\mu$ m).

751

752 **Figure 5:** Representative images of small peripheral renal vessels labeled for TH- (green),  
753 CGRP- (red) and SMA-immunoreactivity (blue) A) Right – non-denervated, week 1 [R1]; B)  
754 Left – denervated, week 1 [L1]; C) Right – non-denervated, week 12 [R12]; D) Left –  
755 denervated, week 12 [L12]; Hardly any nerves are visible in L1. L12 looks very similar to R1  
756 and R12. (Scale bar = 200 $\mu$ m).

757

758 **Figure 6: Sympathetic Innervation (pooled observations):** TH-positive GREEN pixel  
759 count/ROI (635 x 635 $\mu$ m) is displayed. *Left panel:* A significant increase on the non-  
760 denervated side was found (R1\_TH vs. R4\_TH and R12\_TH;  $^{\$}P<0.001$ ; [1W-ANOVA-oR]).  
761 *Right Panel:* A significant decrease was observed one week post DNX (R1\_TH vs. L1\_TH;  
762  $*P=0.0001$ ; [2W-ANOVA-aRT]), which recovered to the “R1\_TH-level” by week 4 and 12  
763 (R1\_TH vs. L4\_TH & L12\_TH;  $P\geq 0.249$ ; [2W-ANOVA-aRT, 1W-ANOVA-oR]). The TH<sup>+</sup>  
764 pixel counts on the denervated side in week 4 and 12 were significantly lower than on the non-  
765 denervated side (R4\_TH vs. L4\_TH;  $P<0.0001$ ; R12\_TH vs. L12\_TH;  $P=0.006$ ; [2W-  
766 ANOVA-aRT]).

767

768 **Figure 7: Afferent Innervation (pooled observations):** CGRP-positive RED pixel  
769 count/ROI (635 x 635 $\mu$ m) is displayed. *Left panel:* A significant increase on the non-DNX-  
770 side was found (R1\_CGRP vs. R4\_CGRP and R12\_CGRP;  $^{\$}P<0.001$ ; [1W-ANOVA-oR]).  
771 *Right panel:* One week post DNX a significant decrease was observed on the DNX-side  
772 (R1\_CGRP vs. L1\_CGRP;  $*P<0.0001$ ; [2W-ANOVA-aRT]), which recovered to “R1\_CGRP-  
773 level” by week 4 and 12 (R1\_CGRP vs. L4\_CGRP & L12\_CGRP;  $P=0.296$ ; [2W-ANOVA-  
774 aRT, 1W-ANOVA-oR]). The CGRP<sup>+</sup> pixel counts on the DNX-side in week 4 was

775 significantly lower than on the non-denervated right side (R4\_CGRP vs. L4\_CGRP;  
776  $P<0.0001$ ; [2W-ANOVA-aRT]). In week 12 no significant difference was observed  
777 (R12\_CGRP vs. L12\_CGRP;  $P=0.085$ ; [2W-ANOVA-aRT]).

778

779 **Figure 8: TH<sup>+</sup>/SMA<sup>+</sup> ratios (averaged observations).** White bars denote the non-  
780 denervated (non-DNX) kidneys, gray bars denote the denervated (DNX) kidneys. One week  
781 post DNX the TH/SMA ratio significantly decreased ( $*P<0.011$ ; [2W-ANOVA]). It recovered  
782 to “R1\_TH/SMA-level” at week 4 and 12 (R1 vs. L4 and L12\_TH/SMA;  $P=0.162$ ; [2W-  
783 ANOVA, 1W-ANOVA]). The TH/SMA ratio 4 weeks after DNX was lower than on the non-  
784 DNX side ( $*P=0.011$ ; [2W-ANOVA]) and still tended to be lower in week 12 (R12 vs. L12;  
785  $P=0.069$ ; [2W-ANOVA]). The TH/SMA ratio significantly increased on the non-denervated  
786 side (R1 vs. R4 and R12;  $P<0.001$ ; [1W-ANOVA]).

787

788 **Figure 9: CGRP<sup>+</sup>/SMA<sup>+</sup> ratios (averaged observations).** White bars denote the non-  
789 denervated (non-DNX) kidneys, gray bars denote the denervated (DNX) kidneys. One week  
790 post-DNX the CGRP/SMA ratio decreased ( $*P<0.009$ ; [2W-ANOVA]) but recovered to  
791 “R1\_CGRP/SMA-level” by week 4 (R1 vs. L4;  $P=0.244$ ) and surpassed the  
792 “R1\_CGRP/SMA-level” by week 12 (R1 vs. L12;  $P=0.049$ ; [2W-ANOVA, 1W-ANOVA]). In  
793 week 4 the CGRP/SMA ratio was significantly lower on the DNX-side ( $*P=0.009$ ; [2W-  
794 ANOVA]) but not in week 12 (R12 vs. L12;  $P=0.931$ ; [2W-ANOVA]). A significant increase  
795 in CGRP/SMA ratio on the non-DNX-side was observed (R1 vs. R4 and R12;  $P=0.037$ ; [1W-  
796 ANOVA]).

797

798 **Figure 10: CGRP<sup>+</sup>/TH<sup>+</sup> ratios (averaged observations).** White bars denote the non-  
799 denervated (non-DNX) kidneys, gray bars denote the denervated (DNX) kidneys. On the  
800 DNX side the CGRP<sup>+</sup>/TH<sup>+</sup> ratio was shifted towards CGRP (L1 vs. L12;  $P=0.009$ ; [1W-

ANOVA]). No such shift was observed on the non-denervated side (R1 vs. R12;  $P=0.314$ ; [1W-ANOVA]). In week 1 the ratio on the denervated side was significantly lower ( $**P=0.019$ ; [t-test]) and in week 12 it was significantly higher ( $*P=0.044$ ; [t-test]) compared to the non-denervated side). No statistical difference could be detected in week 4 (ns:  $P=0.465$ ; [t-test]).

**Figure 11:** Renal tissue CGRP content: *Left panel:* One week after unilateral surgical denervation (DNX) CGRP content was reduced, but it recovered with re-innervation (Black = non-denervated; White = DNX).  $*P\leq 0.005$  non-denervated vs. DNX. [2W-ANOVA].

*Right panel:* Application of Phenol had no significant effect, CGRP just tended to be lower in week 1 (Gray = non-denervated; White-striped = DNX+Phenol).  $*P<0.002$  non-denervated vs. DNX+Phenol; ns $\geq 0.138$ .

**Figure 12:** Renal tissue norepinephrine (NE) content: *Left panel:* One week after unilateral surgical denervation (DNX) NE content was reduced, but the tissue NE-levels did not recover (Black = non-denervated; White = DNX).  $*P\leq 0.005$ ; non-denervated vs. DNX.

*Right panel:* Application of phenol had no significant effect, NE just tended to be lower in week 1 and 4 (Gray = non-denervated; White-striped = DNX+Phenol).  $*P\leq 0.001$ ; non-denervated vs. DNX+Phenol [2W-ANOVA].

Figure 1

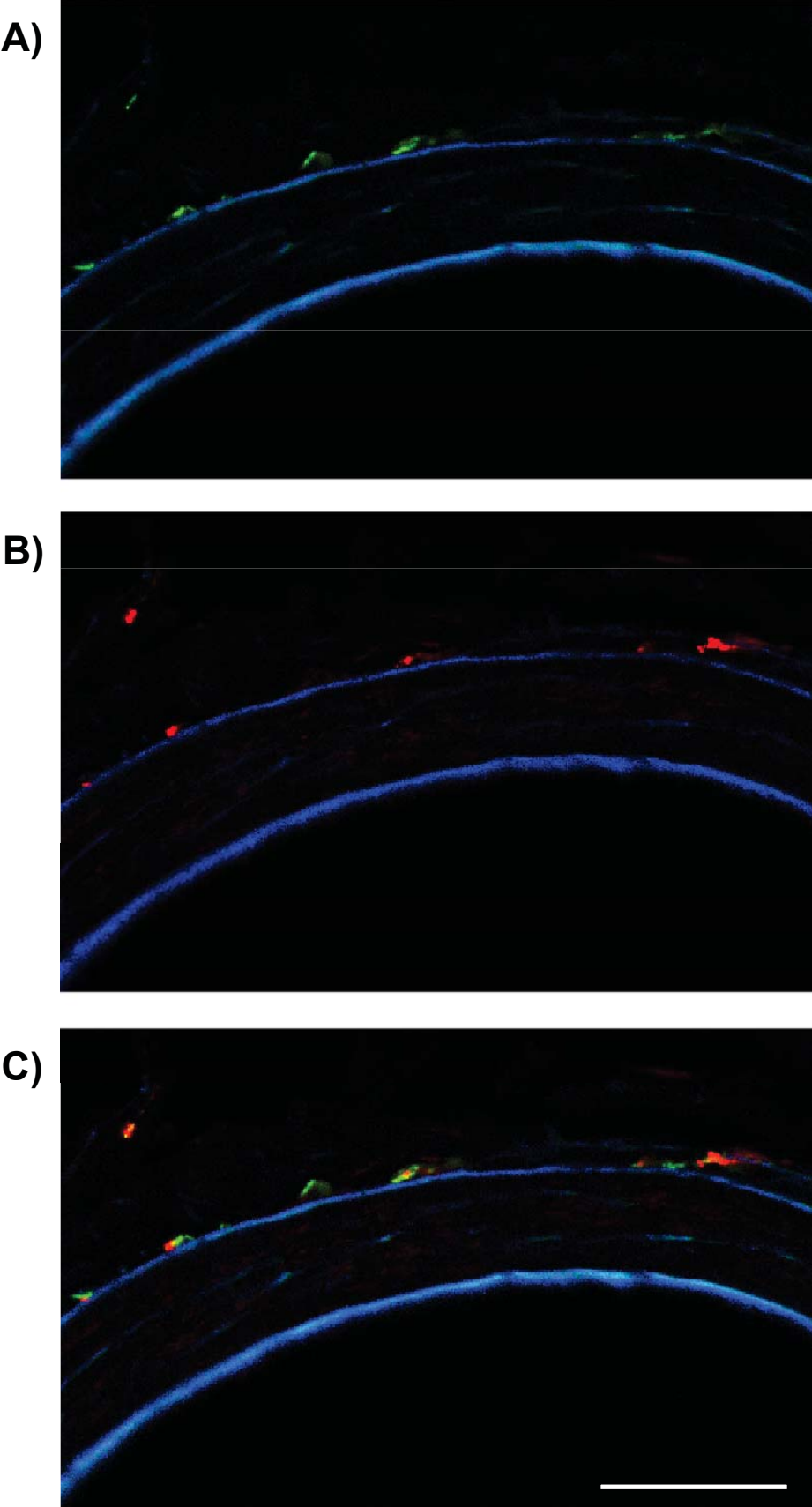
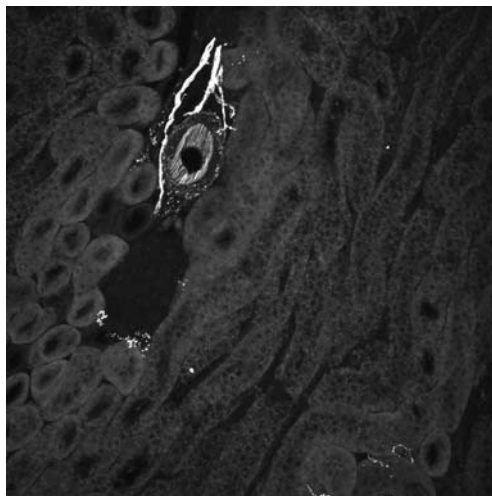




Figure 2

**A)**



**B)**

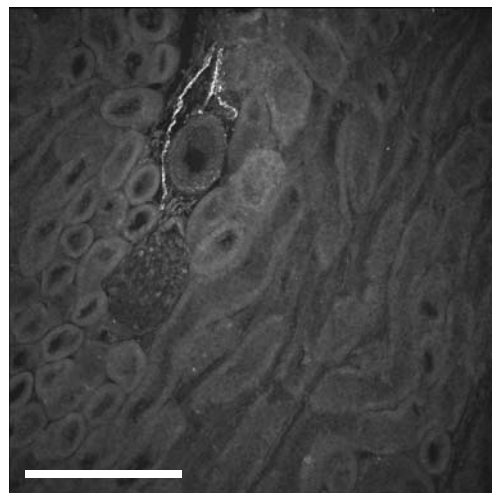


Figure 3

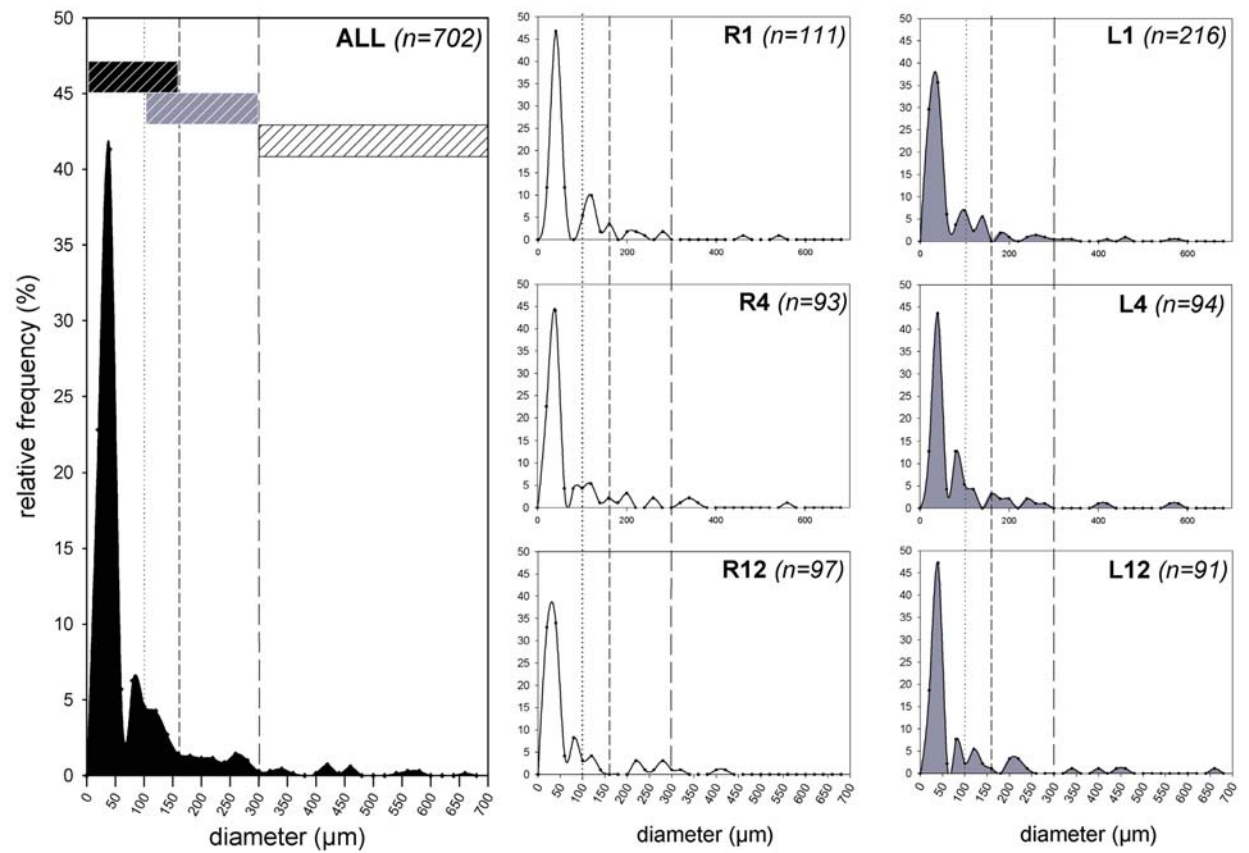


Figure 4

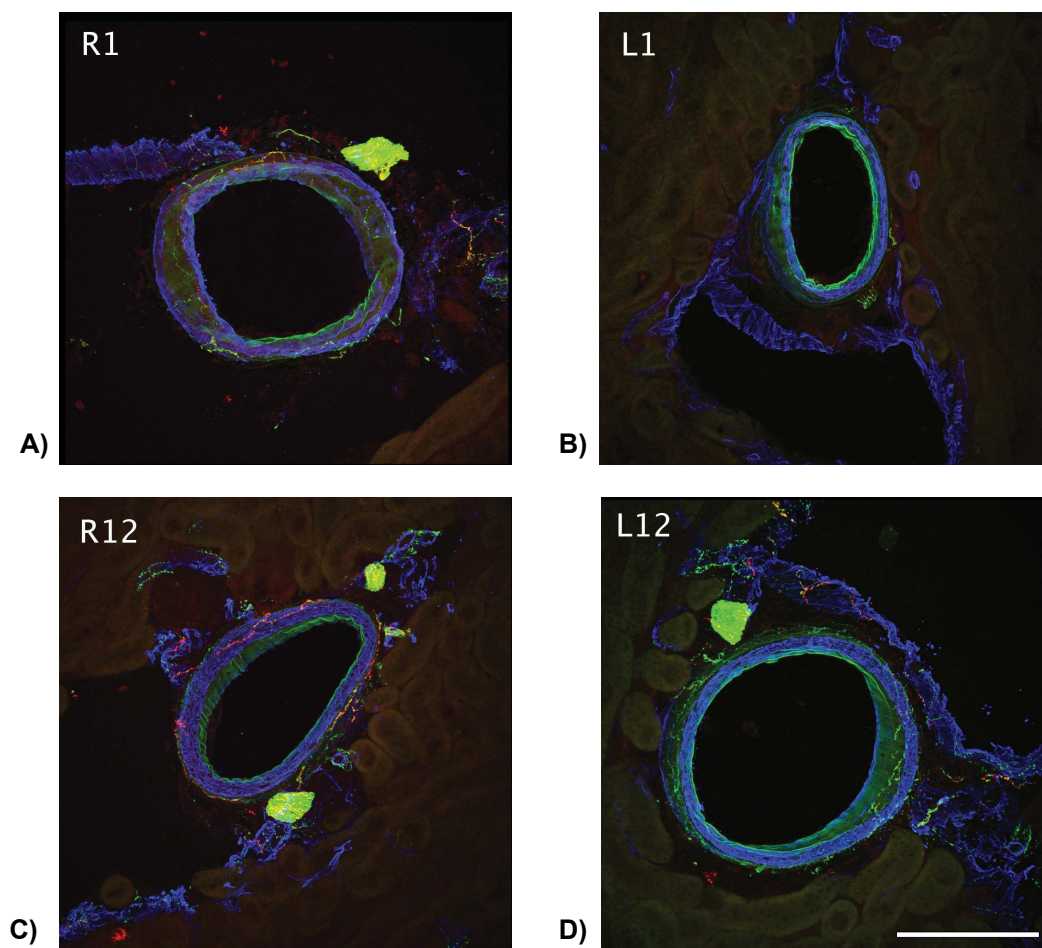




Figure 5

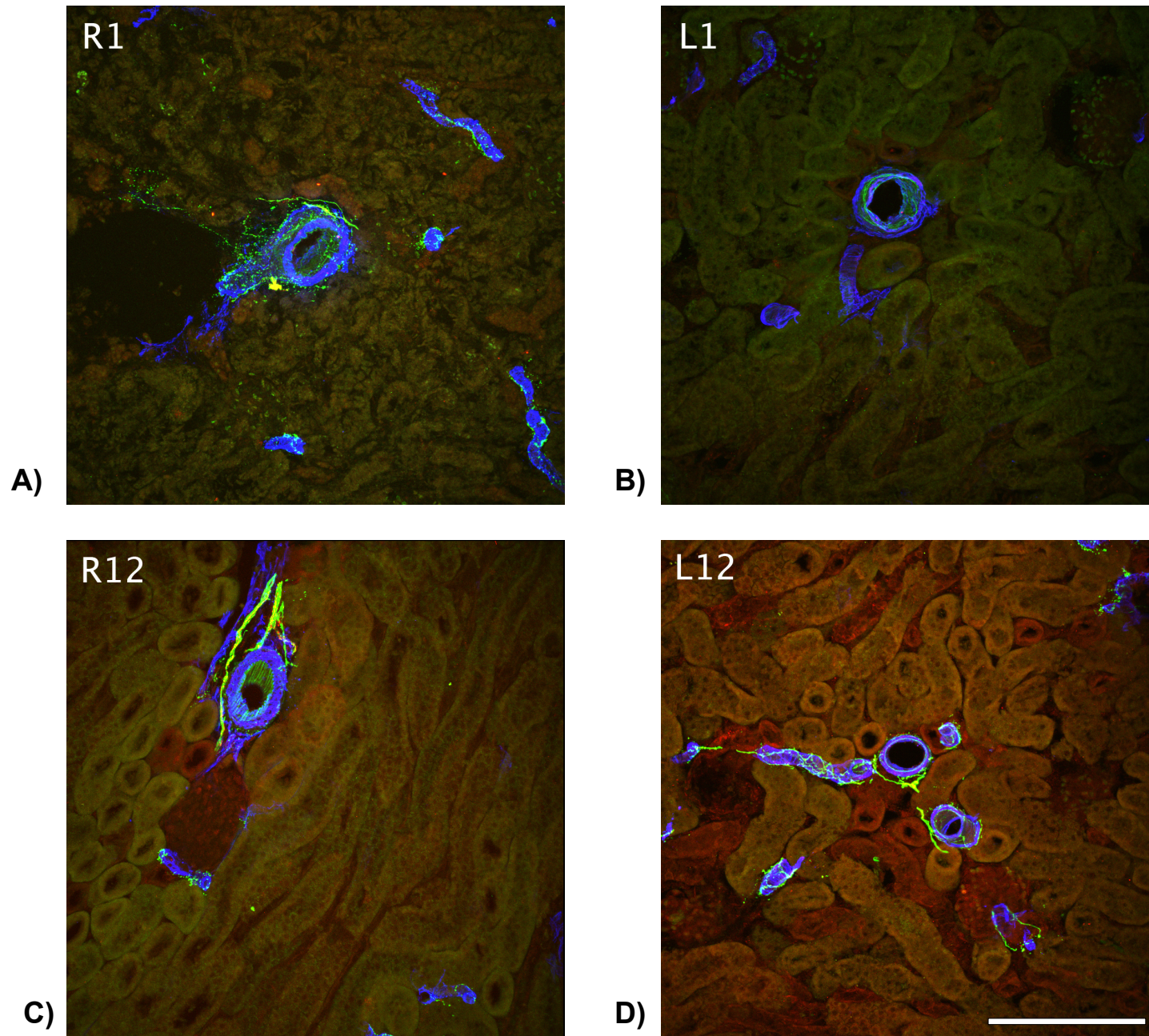


Figure 6

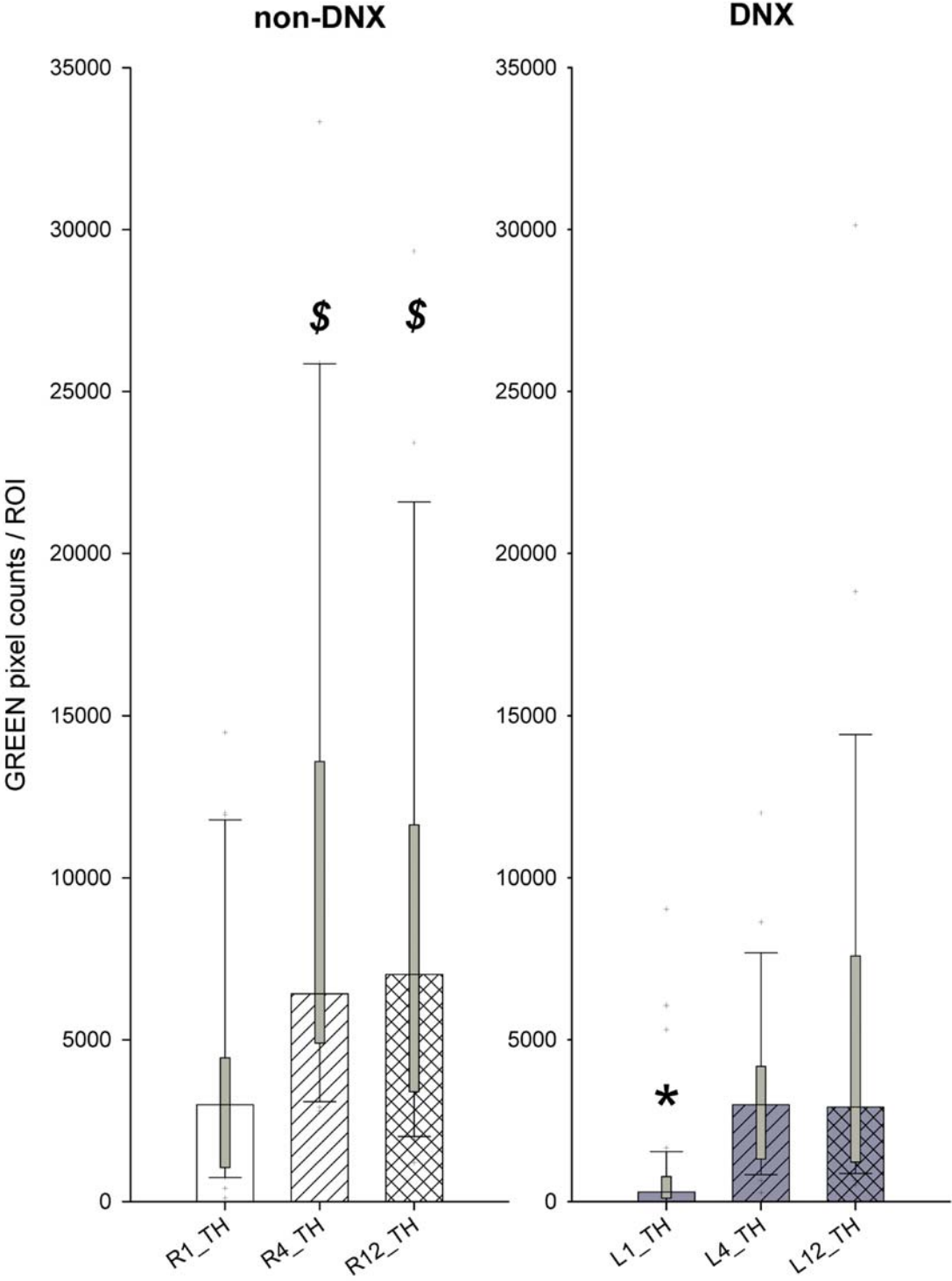


Figure 7

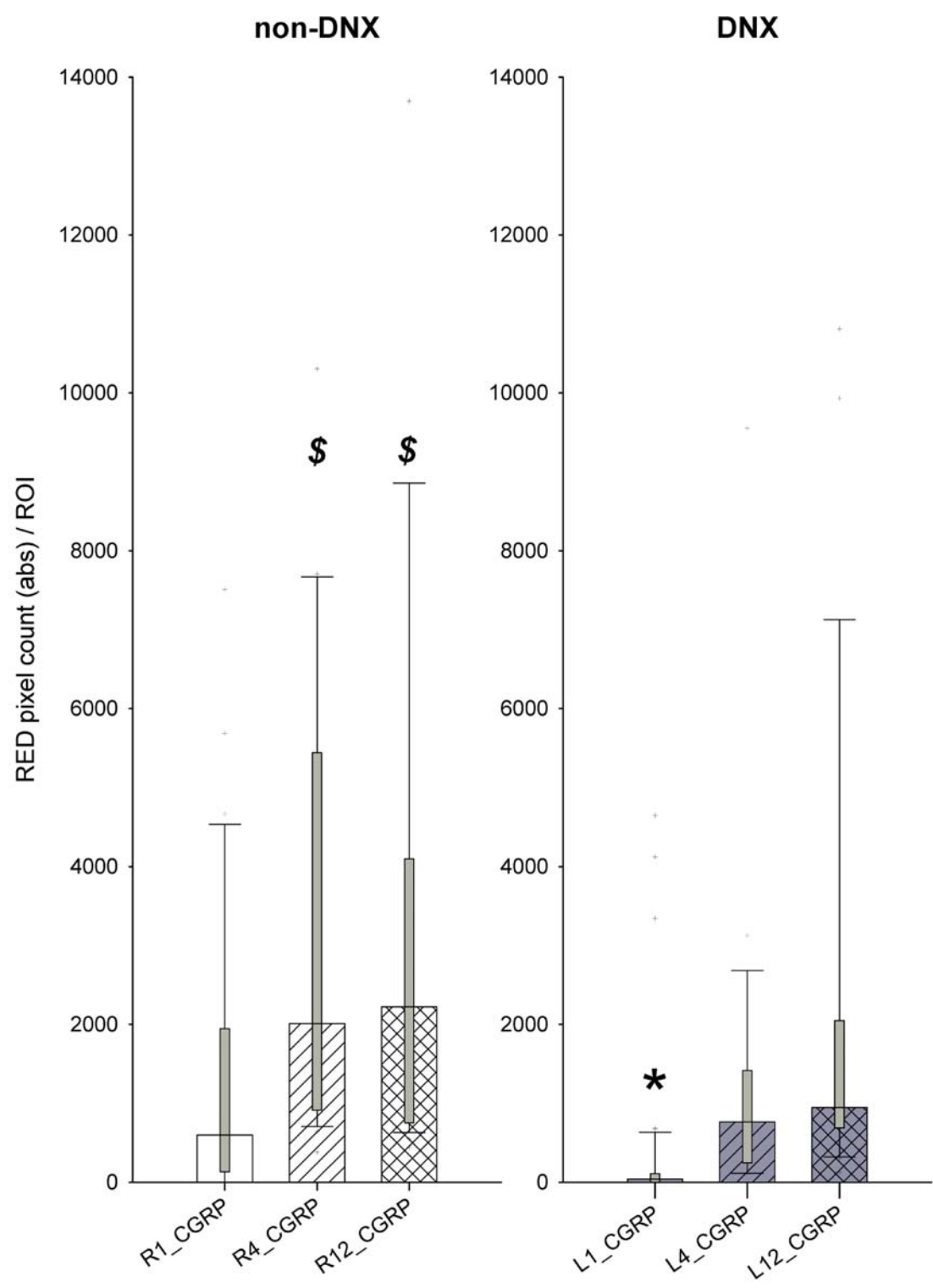


Figure 8

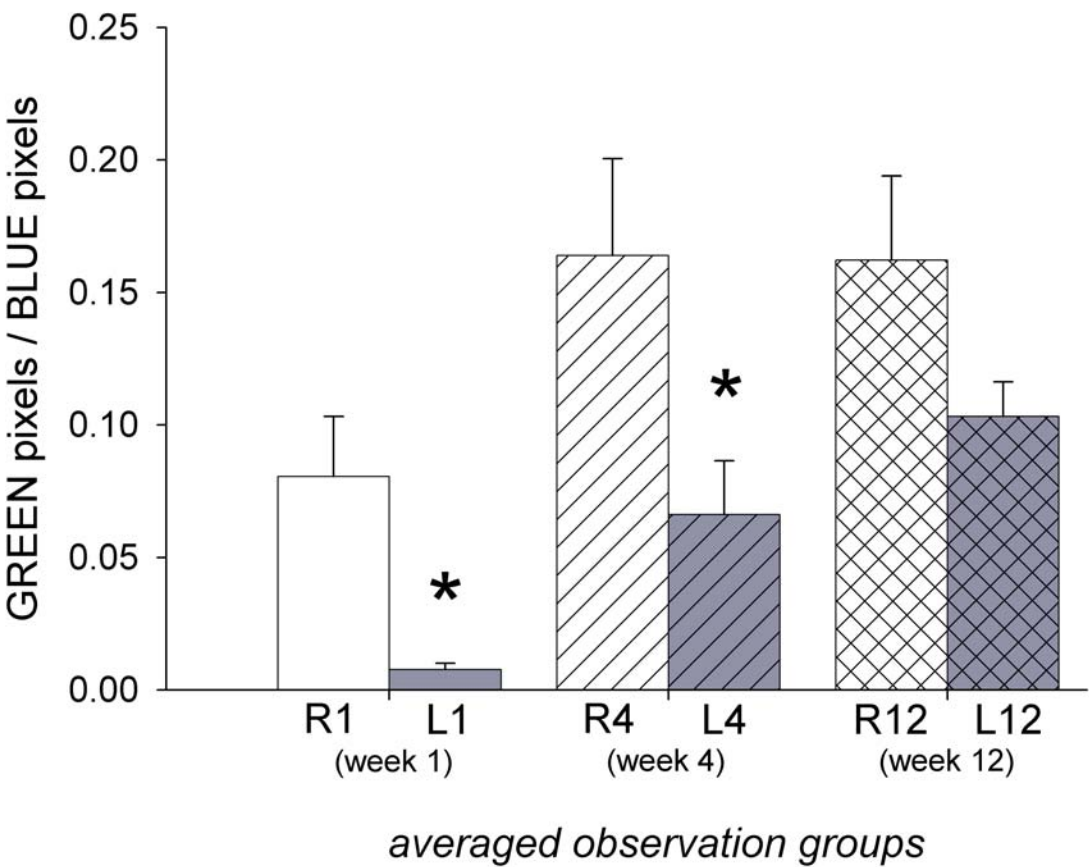


Figure 9

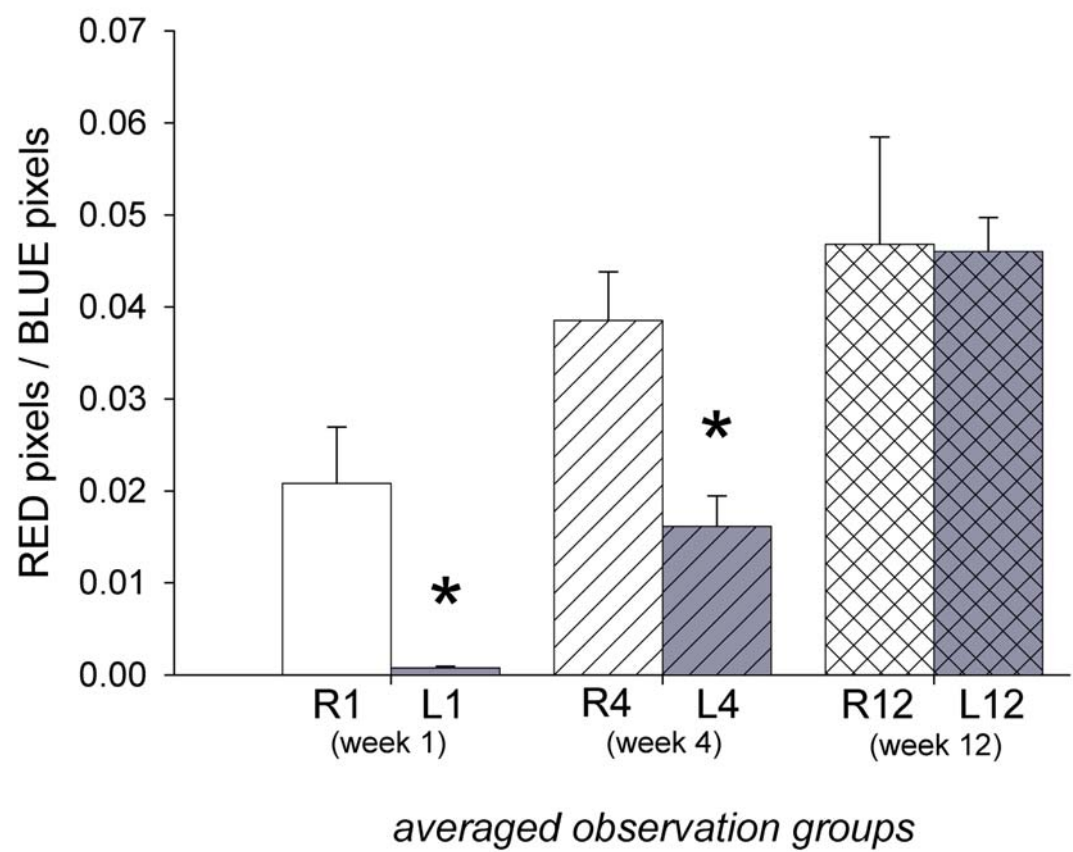




Figure 10

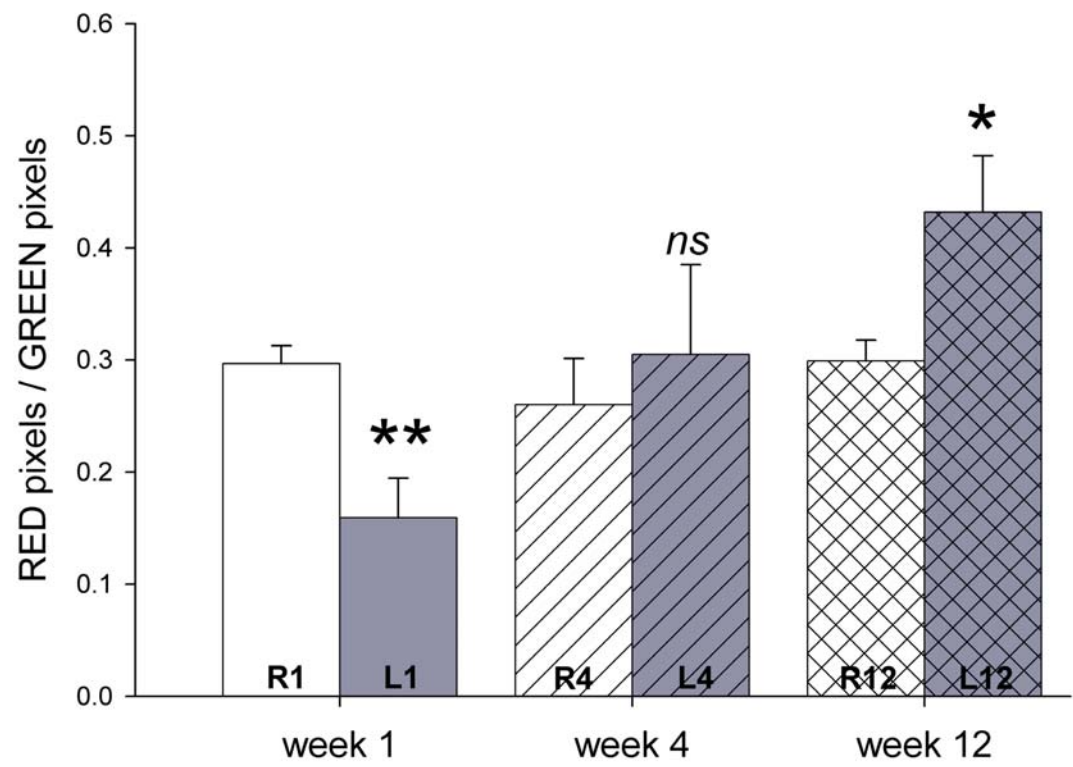


Figure 11

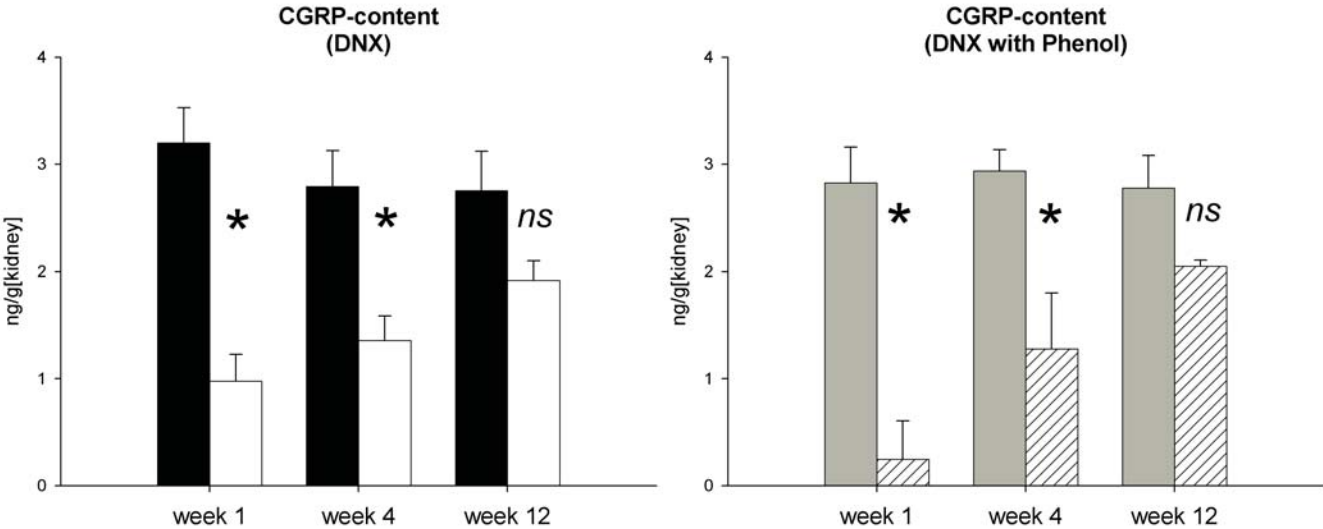


Figure 12

